

# CONTROLHAIR: Physically-based Video Diffusion for Controllable Dynamic Hair Rendering

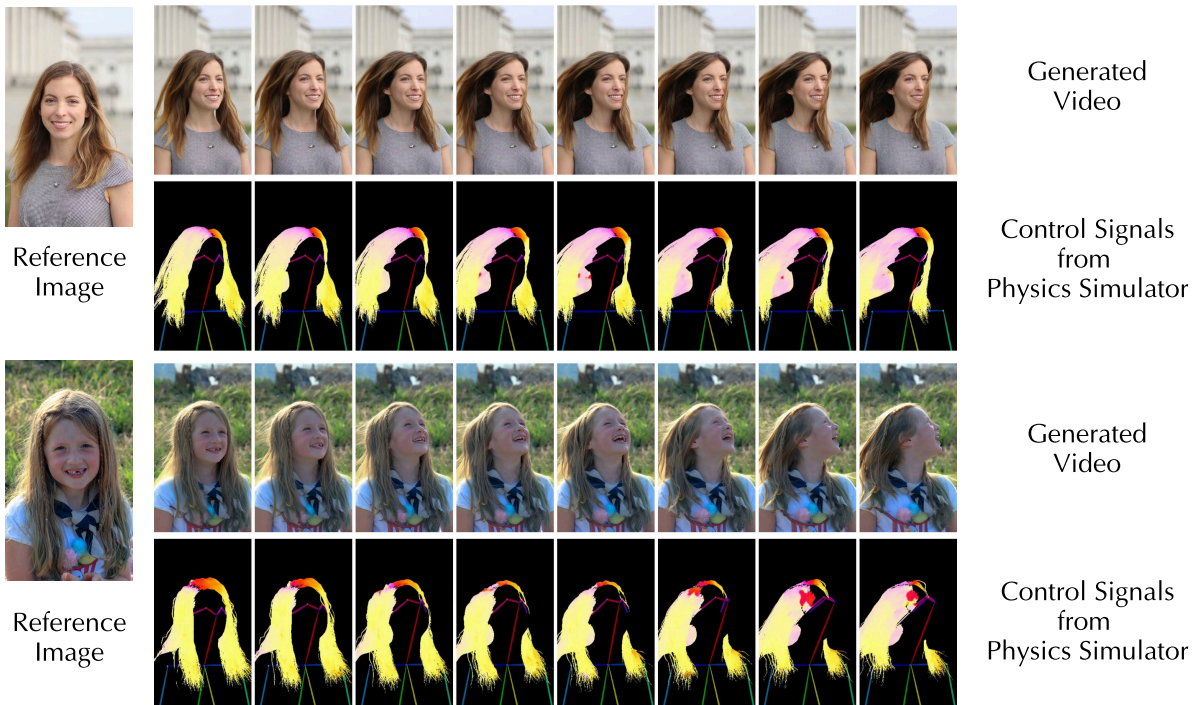
Weikai Lin\*

wlin33@ur.rochester.edu  
University of Rochester

Haoxiang Li

haoxiang@pixocial.com  
Pixocial Technology

Yuhao Zhu

yzhu@rochester.edu  
University of Rochester

**Figure 1:** Given a reference image, CONTROLHAIR converts physics conditions (e.g., hair stiffness, wind, or human motion) into per-frame control signals using a physics simulator. These signals, combined with a reference image, guide a video diffusion model to generate photorealistic videos with controlled hair dynamics.

## Abstract

Hair simulation and rendering are challenging due to complex strand dynamics, diverse material properties, and intricate light-hair interactions. Recent video diffusion models can generate high-quality videos, but they lack fine-grained control over hair dynamics. We present CONTROLHAIR, a hybrid framework that integrates a physics simulator with conditional video diffusion to enable controllable dynamic hair rendering. CONTROLHAIR adopts a three-stage pipeline: it first encodes physics parameters (e.g., hair stiffness, wind) into per-frame geometry using a simulator, then extracts per-frame control signals, and finally feeds control signals into a video diffusion model to generate videos with desired hair dynamics. This cascaded design decouples physics reasoning from video generation, supports diverse physics, and makes training the video diffusion model easy. Trained on a curated 10K video dataset, CONTROLHAIR outperforms text- and pose-conditioned baselines, delivering precisely controlled hair dynamics. We further demonstrate three use cases of CONTROLHAIR: dynamic hairstyle try-on, bullet-time effects, and cinemagraphic. CONTROLHAIR introduces the first physics-informed video diffusion framework for controllable dynamics. We provide a teaser video and experimental results on our [website](#).

## CCS Concepts

- Computing methodologies → **Rendering; Physical simulation; Image-based rendering;**

\* This work was primarily conducted during an internship at Pixocial Technology.

## 1. Introduction

Human hair simulation and rendering are long-standing research problems in computer graphics [PHA05, BWR\*08, HWP\*23, WNS\*23, LOZ\*24], with applications ranging from films and games [IMP\*13, Epi20] to VR/AR and digital humans [XCL\*24, WGL06]. However, hair is exceptionally complex, involving tens of thousands of interacting strands as well as intricate material properties and light scattering. This complexity makes simulation and rendering challenging and computationally demanding.

Video diffusion models [WWA\*25, YTZ\*24, Ope24, KTZ\*24, HCB\*24] have demonstrated the ability to generate high-quality videos rivaling professional production. Beyond common text- and image-conditioned generation, recent works have explored fine-grained and multi-modal controls to enable practical applications. Examples include conditioning on human pose [WZG\*24, MHC\*24, WZT\*25], lighting [YHW\*25], or even speech and music to drive video generation [CCC\*25, THW\*25]. This suggests a promising direction for dynamic hair rendering: one can formulate it as a conditioned generation problem, where physics-related parameters serve as input conditions and the output is a video with corresponding hair dynamics.

However, none of the existing conditional video diffusion methods support fine-grained control over dynamic hair rendering. This limitation arises from two main challenges: (1) There are numerous physics parameters that influence hair dynamics, including intrinsic hair properties (e.g., mass, stiffness, damping) and external forces (e.g., gravity, wind). There is still no general encoding mechanism that can accommodate these diverse conditions. (2) training such conditional models would require videos annotated with ground-truth physics parameters. However, parameters like hair stiffness or wind direction/strength are difficult to infer from videos.

To overcome the above challenges and enable dynamic hair rendering using diffusion models, we first formulate hair simulation and rendering as an image animation problem in the context of conditional video generation (Sec. 3). We then introduce CONTROLHAIR, a video diffusion framework designed for controllable dynamic hair rendering. CONTROLHAIR cascades a physics simulator before the diffusion model, which encodes physics parameters into per-frame geometry. This design brings two benefits. First, it makes CONTROLHAIR general to any physics input because the diffusion model always operates on the same geometry condition from simulator regardless of the physics input. Second, it simplifies training, because we only need to annotate data with per-frame geometry rather than hard-to-infer physical factors such as hair properties or wind fields. CONTROLHAIR is composed of three key components:

**Simulator-based Physics Encoding.** Physics conditions for hair rendering span a wide range of intrinsic parameters and external forces, often specific to the scene, task, or physics model. A straightforward approach is to directly feed these parameters into a diffusion model. However, this introduces two key challenges. First, there may be tens of parameters, making it difficult for the diffusion model to learn the effects of different physics factors. Second, any change in input physics due to different modeling requires redesigning the diffusion model, recollecting training data, and re-training the model, which limits flexibility and generality.

CONTROLHAIR addresses above issues by cascading a physics simulator before the diffusion model. We first estimate a 3D hair model from the input image. The simulator then takes physics parameters as input and use them to generate per-frame hair geometry (Sec. 4.1). This simulation+diffusion hybrid approach has two advantages. First, it offloads dynamics generation to the simulator, relaxing the burden of physics reasoning in the diffusion model. Second, we unify the diffusion model input as per-frame geometry. This decouples the diffusion model from specific physics settings: whenever the physics conditions change, we only need to swap the simulator, without redesigning downstream modules. Overall, our design enhances diffusion models with a physics simulator and supports diverse physics conditions.

**Per-frame Control Signals Extraction.** After obtaining the per-frame hair geometry, we convert it into control signals for the video diffusion model (Sec. 4.2). We first project the 3D geometry onto 2D images along the desired camera trajectory. From these projections, we extract per-frame hair strand maps [ZJL\*23] and human poses [YZYL23] as control signals, which guide the video diffusion model on a per-frame basis. This control-signal design is motivated by three reasons. First, by projecting 3D geometry to 2D, we can control the poses of the generated frames. Second, the chosen strand maps and human poses depend only on geometry, which is available from simulation. Third, these per-frame control signals can be easily extracted from 2D frames in real-world videos, giving us training pairs of control signals and RGB frames. This greatly reduces the difficulty of training data annotation compared to inferring precise 3D geometry or underlying physics.

**Conditioned Video Diffusion for Hair Rendering.** Finally, we design a conditioned video diffusion model that takes a reference image (for appearance) and the per-frame control signals described above to generate desired RGB video (Sec. 4.3). The reference image is encoded using Wan encoder [WWA\*25], while the per-frame control signals are encoded with a dedicated 3D convolution neural network, similar to UniAnimate-DiT [WZT\*25]. For training, we collect a large set of high-quality real-world videos containing hair and annotate them with strand maps and human poses to construct input control signals. The reference image is sampled from the video. The model is then trained to map the reference image and control signals to RGB videos. To leverage the prior of pretrained models, we finetune our backbone from UniAnimate-DiT [WZT\*25] using LoRA [HSW\*21], which adapts the model by adding only low-rank components to the weight matrices.

Experiments show that CONTROLHAIR outperforms existing video diffusion baselines in controllable dynamic hair rendering. We further showcase its broad applicability with diverse use cases, including dynamic hair try-on, bullet-time effects, and cinematic animation. Our contributions are summarized as follows:

- We formulate controllable dynamic hair rendering as a conditional video generation problem with physics inputs.
- We introduce CONTROLHAIR, the first video diffusion framework that incorporates a physics simulator to support flexible and fine-grained physics control.
- We design a control signals extraction pipeline that bridges simulators and diffusion models, enabling pose control and simplifying training data annotation.

- We design a conditional video diffusion model for hair rendering and construct a large-scale, high-quality dataset for training.

We plan to release code and models to facilitate future research.

## 2. Related Work

### 2.1. Video Diffusion Models

Video diffusion has achieved significant quality improvements through both data and computational scaling. Starting from Sora by OpenAI [Ope24], a series of powerful closed-source models have been released by major tech companies, such as Runway Gen-3 [Ger24], Pika 1.5 [Pik24], Meta Movie Gen [PZB\*24], ByteDance Seedance [GGH\*25] and Google Veo3 [Goo25]. On the other side, the open-source community has also made substantial progress, with high-quality video diffusion models such as HunyuanVideo [KTZ\*24], LTX-Video [HCB\*24], CogVideoX [YTZ\*24], Open-Sora [ZPY\*24], and Open-Sora Plan [LGC\*24]. Among them, the Wan series [WWA\*25] has achieved extraordinary quality, even on par with their closed-source counterparts. Our diffusion model builds on the Wan 2.1 architecture. We support controllable dynamic hair rendering by modifying its input and output interfaces and adding extra encoder modules.

### 2.2. Controllable Video Diffusion

Text and image conditions are the most common forms of conditions in pretrained video diffusion models; however, they often fail to capture complex, multi-modal, and fine-grained user requirements. To address this limitation, recent works incorporate additional control signals to guide the generation process. For example, pose-guided generation enables controllable human motion [WZG\*24, MHC\*24, WZT\*25], sketch-guided generation preserves desired structural layouts [XLX\*24, JCW\*25], camera-trajectory control enables cinematic effects [HXG\*24], and audio-guided generation supports speech- or music-driven videos [CCC\*25, THW\*25]. Other aspects of controllable video generation have also been explored, such as style [YHW\*25] and lighting [LGL\*25] control. These advances have unlocked a wide range of control modalities, greatly expanding the applicability of video diffusion. However, none of the existing studies investigate control over the *physical dynamics* of fine structures such as human hair. Our work falls within the scope of controllable video diffusion, but uniquely combines video diffusion with a physics simulator to embed hair-specific physical conditions.

### 2.3. Hair Simulation and Rendering

Human hair simulation and rendering are long-standing challenges in computer graphics. Simulation must account for tens of thousands of interacting strands, while rendering requires handling complex materials and light-scattering effects.

A wide variety of physics simulation methods have been proposed for hair dynamics, such as mass-spring chains [RCTI91], rigid multi-body chains [AUK92], discrete elastic rods [BWR\*08], Material Point Method [FHG21], hybrid approaches [HWP\*23], and learning-based methods [LLC\*25]. These simulations are built

Condition	Examples
Reference image	Image with human, hair, and environment lighting
Hair properties	Mass, Stiffness, Damping, Thickness, etc.
External forces	Wind, Gravity, Friction, Human motion, etc.
Camera trajectory	Camera pose for each frame, Viewpoint changes, etc.

**Table 1:** Input conditions for conditional video generation.

on different physics models tailored for different tasks. Ideally, we should select the most suitable model given a task. However, the diversity of physics parameters across models makes it difficult to design a single diffusion model for all possible physics parameters input. For hair rendering, prior works have explored physically based models [PHA05, MJC\*03, MWM08, ZYWK08], as well as data-driven methods [WNS\*23, LOZ\*24]. However, they either require complex modeling or fail to produce photorealistic results.

Our framework is compatible with arbitrary physics parameters and simulators because we unify the diffusion model input as per-frame geometry. This allows us to switch freely across different simulation models for a given task without redesigning the diffusion model. For hair rendering, we adopt video diffusion priors to avoid complex hair material and light modeling, while producing photorealistic and temporally consistent results.

## 3. Problem Formulation

We first formulate dynamic hair rendering within a conditional video generation framework. This formulation extends naturally to physics-conditioned generation of other deformable objects. Concretely, we model it as image animation problem: the inputs include a reference image  $I_{\text{ref}}$ , physics parameters  $\mathcal{P}$ , and a camera trajectory  $\mathcal{T}_{\text{cam}}$ . The output is a video  $V$  that preserves the reference appearance while following the dynamics dictated by  $\mathcal{P}$  and camera trajectory defined by  $\mathcal{T}_{\text{cam}}$ , which can be written as:

$$V = \mathcal{G}(I_{\text{ref}}, \mathcal{P}, \mathcal{T}_{\text{cam}}) \quad (1)$$

Here,  $\mathcal{G}$  denotes the conditional video generator.

We now specify the physics parameters  $\mathcal{P}$  that govern hair dynamics. We categorize them into two groups: intrinsic hair properties ( $\mathcal{P}_{\text{hair}}$ ) and external forces ( $\mathcal{F}$ ). The former characterizes hair geometry and physical attributes that determine how strand responses to external stimuli (e.g. mass, stiffness). The latter captures external forces in the scene such as wind or gravity. We summarize the conditions and examples in Tbl. 1. Note that the physics parameters  $\mathcal{P}$  are not fixed, as they depend on the task and the underlying physical modeling principles. Formally, we can rewrite the formulation in Eqn. 1 as:

$$V = \mathcal{G}(I_{\text{ref}}, \mathcal{P}_{\text{hair}}, \mathcal{F}, \mathcal{T}_{\text{cam}}) \quad (2)$$

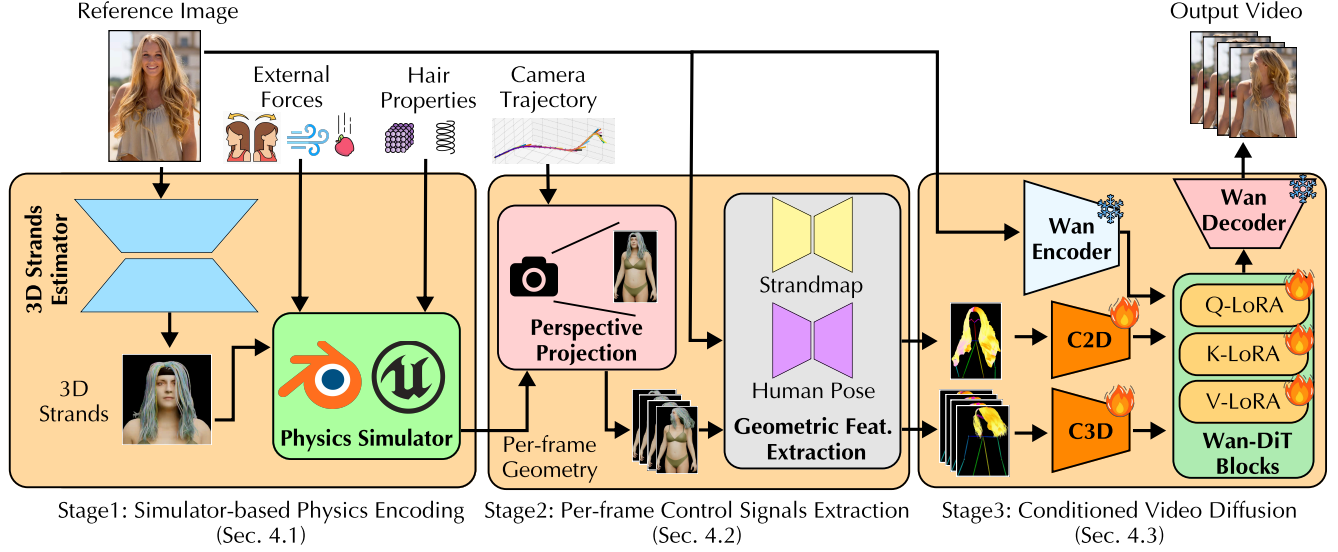


**Figure 2: Overview.** CONTROLHAIR for controllable dynamic hair rendering consists of three stages: (1) Simulator-based Physics Encoding (Sec. 4.1), (2) Per-frame Control Signal Extraction (Sec. 4.2), and (3) Conditioned Video Diffusion for Hair Rendering (Sec. 4.3).

The formulation indicates that the generator  $\mathcal{G}$  must fuse  $I_{\text{ref}}$ ,  $\mathcal{P}_{\text{hair}}$ ,  $\mathcal{F}$ , and  $\mathcal{T}_{\text{cam}}$  to produce a video in which appearance, hair dynamics, and camera motion are faithfully controlled. However, directly feeding these conditions into  $\mathcal{G}$  makes generation difficult. To address this, people usually employ some form of encoder that transforms the conditions into control signals better suited for  $\mathcal{G}$ . For instance, one of the most widely adopted approaches, ControlNet [ZRA23], unifies all conditions into control signals that share the same shape as the target output, i.e., the video  $V$  in our formulation. Based on this idea, we can rewrite Eqn. 2 as:

$$V = \mathcal{G}(E_I(I_{\text{ref}}), E_{\text{hair}}(\mathcal{P}_{\text{hair}}), E_F(\mathcal{F}), E_T(\mathcal{T}_{\text{cam}})) \quad (3)$$

Here,  $E_I$ ,  $E_{\text{hair}}$ ,  $E_F$ ,  $E_T$  denote encoders that transform the corresponding input conditions into control signals consumed by  $\mathcal{G}$ . Prior work has studied encoding the reference image for appearance control [WWA\*25] and encoding camera trajectories for pose control [HXG\*24]. However, accurately encoding dynamics-related physics, such as  $\mathcal{P}_{\text{hair}}$  and  $\mathcal{F}$ , remains unexplored. The difficulty arises because of two reasons: (1) the effects of physics parameters are often highly entangled, making it difficult for a model to disentangle their effects. For example, lower damping, weaker gravity, or stronger wind can all lead to similar visual outcomes, such as elevated hair strands. (2) The parameter set  $\mathcal{P}$  may vary across physics models designed for different tasks, which makes it challenging to design a single diffusion model that handles all inputs. Based on these reasons, an ideal condition encoding mechanism must both ease model learning and remain flexible to accommodate diverse physics inputs.

#### 4. Method

We now introduce CONTROLHAIR. We extend prior image-conditioned [WWA\*25] and human pose-conditioned [WZT\*25]

frameworks to incorporate physics inputs. In CONTROLHAIR, we investigate how to encode physics conditions through a representation that is both general and precise. This design also reduces training data annotation cost. CONTROLHAIR adopts a three-stage pipeline as shown in Fig. 2. First, we encode physics conditions into per-frame hair geometry using a physics simulator (Sec. 4.1). Second, we extract per-frame control signals by (1) projecting the geometry onto the 2D image along the desired camera trajectory and (2) extracting strand maps and sparse human poses (Sec. 4.2). Finally, the per-frame control signals, together with the reference frame, are fed into a conditional video diffusion model to generate the output video (Sec. 4.3).

We can also map stages in CONTROLHAIR to Eqn. 3. The first two stages encode physics conditions and camera trajectories to produce control signals, corresponding to  $E_{\text{hair}}, E_F, E_T$ . The final stage employs  $E_I$  from Wan 2.1 [WWA\*25] to encode the reference image and uses a conditional video diffusion model as  $\mathcal{G}$  that jointly processes all encoded control signals. We describe each stage of the pipeline in detail below.

#### 4.1. Simulator-based Physics Encoding

**Motivation.** Encoding physics into video generation is challenging. First, many parameters have highly entangled effects. For example, decreasing hair mass, increasing wind force, or reducing gravity can all amplify hair motion, making it difficult to disentangle their contributions and learn the correct physics. Second, different target effects often require different physical modelings, which introduce distinct physics parameters. It is therefore difficult to design a universal video diffusion architecture that can handle arbitrary parameters across diverse physics models.

To address the above challenges, CONTROLHAIR cascades a physics simulator before running video diffusion (Stage 1 in Fig. 2). The simulator takes as input user-defined physics parameters, i.e.,

intrinsic hair properties and external forces (Tbl. 1), together with a 3D hair strand model estimated from the reference image. It then performs time-step simulations on the 3D hair model to infer per-frame hair geometry. The process can be formulated as:

$$H_{1:T} = \mathcal{S}(H, \mathcal{P}_{\text{hair}}, \mathcal{F}), \quad (4)$$

Here,  $H$  is the 3D hair model estimated from the reference image,  $\mathcal{P}_{\text{hair}}$ ,  $\mathcal{F}$  represent hair intrinsic properties and external forces, respectively, and  $\mathcal{S}$  is a physics simulator compatible with  $H$ ,  $\mathcal{P}_{\text{hair}}$ , and  $\mathcal{F}$ .  $H_{1:T}$  is per-frame hair geometry over  $T$  frames.

We support  $\mathcal{P}_{\text{hair}}$  by configuring hair-related physical parameters in the simulator. For external forces  $\mathcal{F}$ , standard settings cover most cases, such as wind strength/direction and gravity. To account for the effect of human motion (a component of  $\mathcal{F}$ ) on hair dynamics, we instantiate a digital human in the simulator, attach hair strands to its scalp, and drive the character with the desired motions. This setup allows human motion to directly influence hair behavior. The simulator finally outputs  $H_{1:T}$ . The  $H_{1:T}$  is then encoded into per-frame control signals (Sec. 4.2), which will be used to guide the video generation (Sec. 4.3). Note that we are free to switch among different simulators ( $\mathcal{S}$ ) and physics conditions ( $\mathcal{P}_{\text{hair}}$ ,  $\mathcal{F}$ ) as long as the output of the simulator is per-frame hair geometry.

This cascaded, decoupled design offers two key advantages. First, it delegates the main part of physics-based dynamics generation to the simulator, leaving the video diffusion model to focus on photorealistic inpainting based on simulated geometry, thereby reducing its burden of physics reasoning. Second, it unifies diverse physics parameters into a common representation: per-frame hair geometry. As a result, users can modify the parameter set for different tasks simply by switching to a suitable simulator, without altering the downstream design. However, estimating 3D hair strands from a single image may introduce geometric errors, as it is an under-constrained problem. These errors could propagate into the generated video. Fortunately, we observe that the diffusion model, guided by the reference image, often corrects mismatches caused by this imperfect reconstruction. We further discuss this in Sec. 6.

## 4.2. Per-frame Control Signals Extraction

After obtaining per-frame hair geometry from the simulator, we convert it into control signals for video diffusion. Here, the inputs are the simulated hair geometry  $H_{1:T}$  from Stage 1. and a human model sequence  $M_{1:T}$ , defined by the sequence of human motion poses in  $\mathcal{F}$ . This stage then outputs per-frame control signals for the video diffusion model, which control both hair dynamics and human motion. Inspired by recent controllable generation [ZRA23, WZG\*24, WZT\*25], we define the control signals to have the same shape as the output video ( $T \times H \times W$ ), thereby providing pixel- and frame-wise control.

We impose two requirements on the control signals: (1) they must reflect the desired camera trajectory  $T_{\text{cam}}$  to allow camera pose control, and (2) they should depend only on geometry, as the physics simulator produces purely geometric results. CONTROLHAIR generates the control signals in two steps: (1) trajectory-aware 3D-to-2D projection and (2) geometric feature extraction.

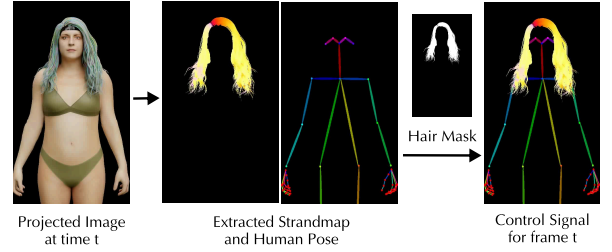


**Figure 3:** Example of extracting control signals from a projected image. These control signals are then fed into the diffusion model.

(Stage 2 in Fig. 2). The first step ensures that the camera trajectory is encoded, and the second ensures that the control signals depend only on geometry.

**Trajectory-aware perspective projection.** To generate the control signal for frame  $t$ , we first project the hair geometry and the 3D human model at time  $t$  to 2D image according to the camera pose  $T_{\text{cam},t}$ , producing a projected image  $I_{\text{proj},t}$ . Formally:

$$I_{\text{proj},t} = \Pi(H_t, M_t; T_{\text{cam},t}) \quad (5)$$

Here,  $\Pi(\cdot)$  denotes the perspective projection, which projects 3D objects onto a 2D image with the same resolution as the target video.  $H_t$  is the simulated hair geometry at time  $t$ , and  $M_t$  represents the human model at time  $t$ , defined by the human pose at time  $t$ . This operation is applied to all frames along the camera trajectory, yielding  $I_{\text{proj},1:T}$ . This design enables explicit control over camera pose, as validated by the bullet-time effect in Fig. 7.

**Geometric feature extraction.** After obtaining the sequence  $I_{\text{proj},1:T}$ , we extract geometric features as control signals. For hair, we use strand map [ZJL\*23], which resemble orientation map but disambiguate directional conflicts and are smoothed by using a neural network as estimator. For human pose, we adopt sparse 2D dw-pose encodings [YZYL23]. These features are then merged into a single RGB control image using a hair mask  $B_{\text{hair}}$ , which is a binary mask indicating regions where hair occludes the human model. Formally, the geometric extraction  $G$  can be written as:

$$C_t = G(I_{\text{proj},t}) = \Phi_{\text{strand}}(I_{\text{proj},t}) \cdot B_{\text{hair}} + \Phi_{\text{pose}}(I_{\text{proj},t}) \cdot (1 - B_{\text{hair}}) \quad (6)$$

Here,  $\Phi_{\text{strand}}(\cdot)$  and  $\Phi_{\text{pose}}(\cdot)$  denote the feature extraction processes for strand map and human pose, respectively, both are neural networks in our implementation.  $C_t$  is the control signal for frame  $t$  which has same resolution as the output video. We show an example of control signal extraction in Fig. 3. We obtain  $C_{1:T}$  by applying this extraction to all projected frames  $I_{\text{proj},1:T}$ , which serve as per-frame control signals for video diffusion model (Sec. 4.3).

## 4.3. Conditioned Video Diffusion for Hair Rendering

With the per-frame control signals  $C_{1:T}$  and the reference image  $I_{\text{ref}}$ , we employ a conditional video diffusion model  $\mathcal{G}$  to generate the output video  $V_{1:T}$  (Stage 3 in Fig. 2):

$$V_{1:T} = \mathcal{G}(E_I(I_{ref}), E_{C3D}(C_{1:T}), E_{C2D}(G(I_{ref}))) \quad (7)$$

Here,  $C_{1:T}$  provides frame-wise geometric constraints, while the reference image  $I_{ref}$ , encoded by  $E_I$ , specifies appearance constraints. We use Wan 2.1 encoder [WWA<sup>25</sup>] as  $E_I$ . Before feeding the control signals into the diffusion backbone, we encode them using a 3D convolutional network  $E_c$ . In addition, we extract geometric features (Eqn. 6) from the reference image, encode them with a 2D convolutional network  $E_{c2d}$ , and inject them into the diffusion model. This design bridges the modality gap between the reference image and the control signals. This encoding design follows previous controllable diffusion models [ZRA23, WZG<sup>24</sup>, WZT<sup>25</sup>]. All encodings are then fed into a Wan 2.1 diffusion transformer (DiT), which generates the output video with hair dynamics and human poses faithfully controlled.

**Data Annotation Made Easy.** No existing diffusion model supports our control signals. To address this, we fine-tune a pretrained model with paired control signals and RGB videos. Through this training, the model learns to map control signals, together with a reference image, into video. To obtain such data, we annotate RGB videos with control signals and sample one frame from each video as the reference image. Specifically, we run geometric feature extraction (Eqn. 6) on every video frame, with  $B_{hair}$  estimated by a hair segmentation network. This gives us the control signals. We show annotation examples in Fig. 4. CONTROLHAIR makes training data annotation easier than directly using physics parameters, because inferring underlying physics from videos is challenging. To enable high-quality training, we collect 30K real-world videos containing hair. We crop each video to focus on the upper body and hair, and filter samples by resolution and aspect ratio. After annotation, we obtain a curated dataset of 10K high-quality videos.

**Training.** To leverage priors from pretrained diffusion models, we initialize our model with pretrained weights from UniAnimate-DiT [WZT<sup>25</sup>] and fine-tune it with our annotated dataset to learn the mapping from new control signals to videos. During training, we keep the Wan encoder and decoder [WWA<sup>25</sup>] fixed. We fully fine-tune only the convolutional networks. For the DiT backbone, we apply LoRA [HSW<sup>21</sup>], which adapts the model by adding only low-rank components to the weights. This choice is motivated by the fact that the DiT backbone contains most of the parameters and prior knowledge; using low-rank fine-tuning not only reduces computation but also prevents overfitting to our dataset.

## 5. Evaluation

### 5.1. Experimental Setup

**Dataset.** We train CONTROLHAIR on a curated dataset of 10K videos (Sec. 4.3). For image animation evaluation, we use public internet images and FFHQ-Wild [KLA19], a high-quality human image dataset. We focus on images with medium or long hair to better assess the model’s ability to capture rich hair dynamics, since the dynamics of short hair are minimal. For control-signal-to-video reconstruction (Sec. 5.3), we generate ten videos with hair dynamics driven by wind or human motion using Google VEO 2 [Goo25], ensuring they are unseen by the evaluated models.

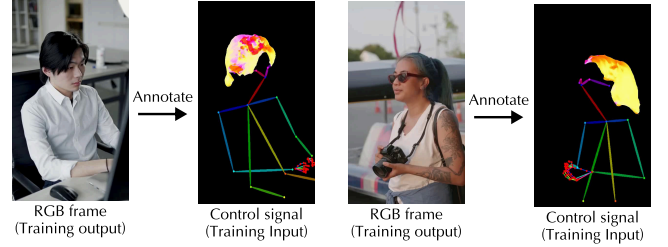


**Figure 4: Training data annotation.** Extracting our control signals from real-world videos is easier than inferring the physics.

**Implementation Details.** We now describe the design choices of each module shown in Fig. 2:

- In **Stage 1**, we adopt DiffLocks [RWF<sup>25</sup>] to extract 3D hair strands from a single image. For the physics simulator, we use Blender’s particle system [Com18] to simulate hair dynamics. We explicitly configure hair properties such as mass, stiffness, and damping, as well as external forces including wind, human motion, and gravity, while keeping the remaining parameters at their default values. Unless otherwise specified, we set mass = 0.1, stiffness = 6, damping = 9, wind strength = 10, and gravity = 1 (scale factor).
- In **Stage 2**, we use Blender’s camera system for pin-hole projection. The strand maps are extracted with a pretrained U-Net from HairStep [ZJL<sup>23</sup>], and 2D human poses are estimated using DWPose [YZYL23].
- In **Stage 3**, we follow the convolutional network design of UniAnimate-DiT [WZT<sup>25</sup>] and adopt the encoder, decoder, and DiT from Wan 2.1 [WWA<sup>25</sup>]. We set the output video resolution to  $81 \times 832 \times 480$  ( $T \times H \times W$ ) for all experiments.

During training of diffusion model, we fix the encoder and decoder from Wan, fully finetune the convolutional network, and train the DiT with LoRA [HSW<sup>21</sup>] (rank = 128) to enable hair-conditioned video diffusion. Training is performed with a learning rate of  $1 \times 10^{-4}$ , a batch size of 4, and 10K iterations, taking three days on four H100 80GB PCIe GPUs.

**Baselines.** Since no prior work targets physics-conditioned video generation, we compare CONTROLHAIR with two intuitive alternatives: text-conditioned and pose-conditioned generation. The goal is to show that CONTROLHAIR provides more precise and detailed control over physics-driven hair dynamics.

- **WAN2.1** [WWA<sup>25</sup>]: a strong video diffusion model that supports image-to-video generation conditioned on text prompts. We provide detailed text prompts to describe the physics.
- **UNIIMATE-DiT** [WZT<sup>25</sup>]: a image-to-video generation framework conditioned on per-frame human pose and text.

See our [website](#) for video results in this section.

### 5.2. Qualitative Comparison

We evaluate CONTROLHAIR against baselines under two physics settings. Setting 1 applies strong wind to the hair, while Setting 2 applies head motion that induces hair dynamics. The results are shown in Fig. 5.

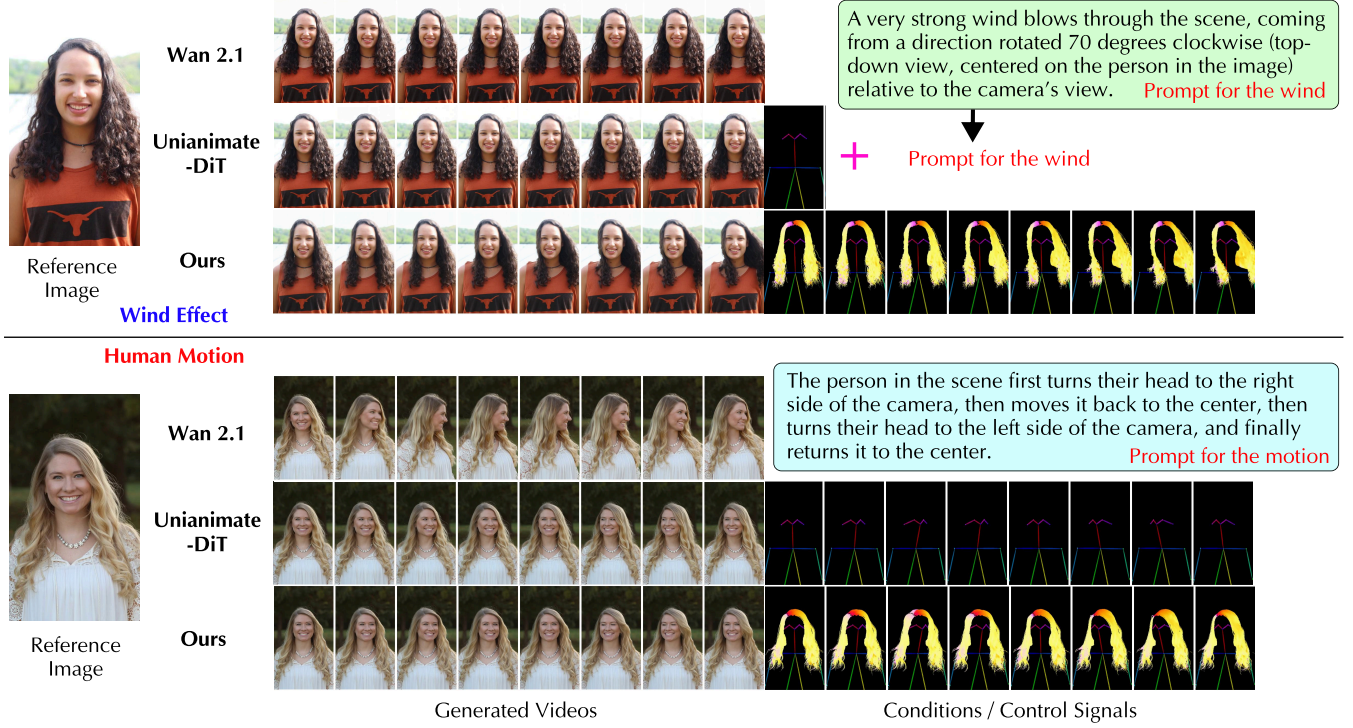


**Figure 5:** Qualitative comparison with baselines under strong wind (top) and human motion (bottom). Only CONTROLHAIR generates realistic strong-wind effects and achieves pixel-level control of hair dynamics.

In Setting 1 (top), we add a strong wind to blow the hair of the reference image. The wind direction is rotated 70° clockwise (top-down view) from the camera view, centered on the person. For the baselines, the only way to represent wind is through text prompts. We provided detailed prompts explicitly describing strong wind effects, as shown in Fig. 5. However, even with aggressive wording (e.g., “strong wind”), both baselines fail to move the hair, highlighting the difficulty of controlling fine-grained physical effects via text conditions. In contrast, CONTROLHAIR leverages control signals from a physics simulator and is able to drive hair motion in the expected direction.

In Setting 2 (bottom), the user’s head is required to first rotate to the right of the camera, then to the left, and finally return to the center. We evaluate two aspects: whether the head motion follows the specified sequence, and whether the hair dynamics are controllable. In WAN2.1, we use detailed text prompt shown in Fig. 5. Although the prompt clearly specifies the intended motion, the generated video shows the head turning only to the right but never to the left, violating the required sequence. UNIANIMATE-DiT successfully controls the head pose, as it is conditioned on human poses, however, it cannot control hair dynamics and instead relies solely on the diffusion prior. In contrast, CONTROLHAIR achieves accurate control of both head motion and hair dynamics by following simulator-provided signals, yielding more controllable results.

### 5.3. Quantitative Comparison

We now evaluate qualitatively how well our diffusion model can leverage and follow the control signals. We use the control-signal-

**Table 2:** Quantitative comparison between generated and ground-truth results. Results are averaged across 10 videos.

Method	PSNR $\uparrow$	SSIM $\uparrow$	LPIPS $\downarrow$
Wan 2.1 [WWA*25]	11.65	0.518	0.499
UniAnimate-DiT [WZT*25]	15.78	0.637	0.390
<u>CONTROLHAIR</u> (Ours)	<b>17.15</b>	<b>0.668</b>	<b>0.370</b>

to-video reconstruction task, which is widely adopted in prior controllable generation works [WZG\*24, Hu24, KHWKS23]. Specifically, we treat videos generated by Google VEO 2 [Goo25] as ground truth (the user-expected video) and extract control signals from them, which are then used to reconstruct the original videos. For WAN2.1, we use the text prompts provided to VEO 2 plus manually annotated human motion (in text) as control signals. For UNIANIMATE-DiT, control signals include the text prompts provided to VEO 2 and per-frame human poses extracted using DW-Pose [YZYL23]. For CONTROLHAIR, control signals include per-frame human poses and hair strand maps, which is extracted using Eqn. 6. We aim to test whether each model can follow the control signals to reconstruct the expected video. This demonstrates how well the generation process is controlled.

The results are shown in Tbl. 2, where we compare the generated and ground-truth videos using widely adopted frame-similarity metrics: PSNR [HTG08], SSIM [WBSS04], and LPIPS [ZIE\*18]. The results are averaged across all frames in all videos. WAN 2.1 performs the worst, because text prompts cannot precisely cap-



**Figure 6: Dynamic Hair Try-on using CONTROLHAIR.** We cascade CONTROLHAIR after existing static image-based hair try-on frameworks to enable dynamic hair try-on.

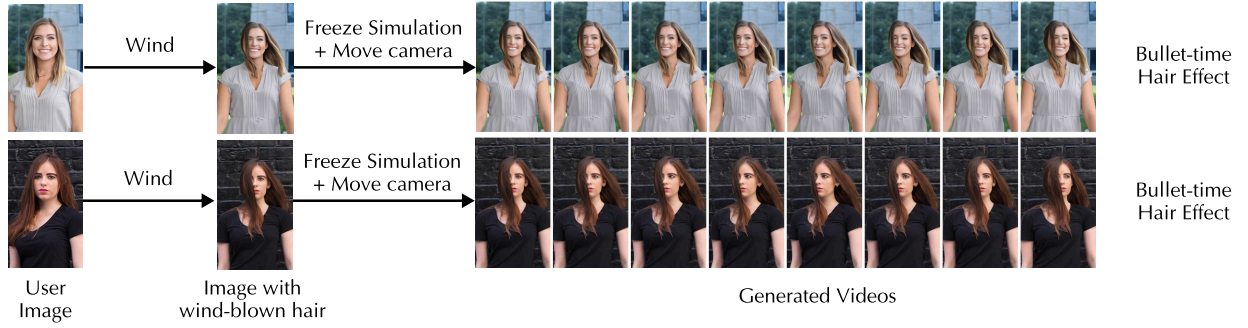


**Figure 7: Bullet-Time Effects.** We freeze the physics simulator and rotate the camera around the user to produce the bullet-time effect.

ture per-frame physics. UNIANIMATE-DiT performs better since it has additional human poses input. Among all methods, CONTROLHAIR achieves the best results, achieving improvements of up to 47%, 29%, and 26% in PSNR, SSIM, and LPIPS, respectively. This indicates: (1) CONTROLHAIR has the highest controllability over generation, and (2) CONTROLHAIR can follow and leverage additional hair-dynamics control signals (strand maps).

#### 5.4. Use Cases

To demonstrate the practicality and broad applicability of CONTROLHAIR, we showcase three representative use cases: dynamic hair try-on, bullet-time hair effects, and cinematographic. We show two examples per use case.

**Dynamic Hair Try-On.** Hair try-on is an important task: it allows users to preview whether a hairstyle suits them before making changes. However, prior work has focused only on static try-on [ZZS<sup>25</sup>, CPKC25], limiting users' understanding of how a hairstyle appears in dynamic scenarios. To enable dynamic hair try-on, we cascade CONTROLHAIR after a prior static hair try-on system. We use HairFusion [CPKC25] for the static hair try-on.

The results are shown in Fig. 6. Given a user image and a target hairstyle, we first apply HairFusion to obtain a static try-on image. We then use CONTROLHAIR to introduce dynamics such as head rotations (first row) or wind effects (second row), yielding the final dynamic hair try-on videos. Since HairFusion outputs images with an aspect ratio of 1:1, we crop the generated videos accordingly for

convenient comparison. The results show that by combining CONTROLHAIR with a static try-on system, we extend static hair try-on to dynamic hair try-on with detailed and controllable dynamics.

**Bullet-Time Hair Effects.** As discussed in Sec. 4.2, we can control the camera trajectory of video generation by manipulating the perspective projection. This enables a special effect: at a specific moment of hair dynamics, we can freeze the physics simulator to lock the hair geometry and render the scene from multiple consecutive viewpoints. This produces a bullet-time effect, allowing users to observe the hair from different perspectives at the same instant. To showcase this application, we first apply a left-to-right wind in the physics simulator. We then freeze the resulting hair geometry. After freezing, we rotate the camera around the person: 20° to the right, followed by 40° to the left.

We show the results of the bullet-time effect in Fig. 7. The hair geometry is well frozen, and the scene can be viewed along the desired rotation trajectory (see video on our website). However, since we use only sparse human poses, not all human details are perfectly frozen; for example, facial expressions might still change.

**Cinematographic Effects.** Beyond animating images, CONTROLHAIR can generate rare or unconventional physical effects such as zero gravity, extremely stiff or soft hair, or unusually strong wind. Such effects are difficult to generate using other diffusion models if they are absent from the training data. To showcase this capability, we use CONTROLHAIR to generate videos with cinematographic effects. Specifically, we design the effect such that the human subject remains static while only the hair is animated, and the



**Figure 8:** Cinemagraphic. We animate only the hair and append reverse playback to the video, achieving a cinematographic effect.



**Figure 9:** Auto correction. 3D hair strand estimation from single image may introduce errors, but the video diffusion model often corrects them by leveraging the reference image.

video is looping. Such effect is difficult to capture in the real world, and producing them typically requires complex post-processing.

To achieve this effect, we fix the human pose in the control signals while applying wind to the hair. Looping is enabled by appending a reversed playback segment to the video. The results are shown in Fig. 8, where the model successfully freezes the human while animating the hair. However, because we use sparse human poses in the control signals, this cannot guarantee that all human details are frozen (Sec. 6). Nevertheless, we find that in practice the human remains static with high probability, so with multiple runs (like a lottery), we are likely to yield the desired cinematographic results.

## 6. Discussion and Future Work

CONTROLHAIR enables fine-grained control of physics conditions through its three-stage pipeline (Sec. 4) and supports a variety of special applications (Sec. 5.4).

However, the cascaded framework may also introduce two kinds of errors. First, the 3D hair model estimated from the input image (Stage 1) may be inaccurate, as it is an under-constrained problem. We show an example in Fig. 9, where imperfect hair strand estimation causes the control signals to have shorter hair on the right side. Nevertheless, this error can often be corrected by the video diffusion model using the reference image. As shown in Fig. 9, the diffusion model adjusts the right-side hair length, so the generated video exhibits no noticeable hairstyle change compared to the reference image. Second, the performance of the physics simulator

affects the final results. If the chosen simulator is imperfect, the generated video may look unrealistic.

To mitigate the hairstyle estimation issue, we can leverage foundation models with multi-view priors [GHH\*24, SWY\*23, MAZ\*24, TJW\*23] to generate multi-view images and infer the 3D hairstyle from these views, thereby improving reconstruction accuracy. To achieve realistic simulated dynamics, we can choose suitable physics models depending on the scene or learn a simulator directly from real data [LLC\*25]. We leave these directions as future research.

## 7. Conclusion

In this work, we presented CONTROLHAIR, the first physics-informed video diffusion framework for controllable dynamic hair rendering. Our three-stage pipeline decouples physics reasoning from video generation, integrates physics simulators with conditional video diffusion, and enables fine-grained and flexible control over the dynamics. Trained on a curated 10K dataset, CONTROLHAIR outperforms text- and pose-conditioned baselines in both qualitative and quantitative evaluations. CONTROLHAIR also enables diverse applications, including dynamic hairstyle try-on, bullet-time effects, and cinematographic. The hybrid design proposed in CONTROLHAIR opens new possibilities for embedding physical conditions into generative video models, paving the way toward more controllable and physically grounded rendering.

## References

- [AUK92] ANJYO K.-I., USAMI Y., KURIHARA T.: A simple method for extracting the natural beauty of hair. In *Proceedings of the 19th annual conference on Computer graphics and interactive techniques* (1992), pp. 111–120.
- [BWR\*08] BERGOU M., WARDETZKY M., ROBINSON S., AUDOLY B., GRINSPUN E.: Discrete elastic rods. In *ACM SIGGRAPH 2008 papers*. 2008, pp. 1–12.
- [CCC\*25] CHEN Z., CAO J., CHEN Z., LI Y., MA C.: Echomimic: Lifelike audio-driven portrait animations through editable landmark conditions. In *Proceedings of the AAAI Conference on Artificial Intelligence* (2025), vol. 39, pp. 2403–2410.
- [Com18] COMMUNITY B. O.: Blender - a 3d modelling and rendering package, 2018. URL: <http://www.blender.org>.

[CPKC25] CHUNG C., PARK S., KIM J., CHOO J.: What to preserve and what to transfer: Faithful, identity-preserving diffusion-based hairstyle transfer. In *Proceedings of the AAAI Conference on Artificial Intelligence* (2025), vol. 39, pp. 2582–2590.

[Epi20] EPIC GAMES: An early look at next-generation real-time hair and fur. Unreal Engine Tech Blog, 2020. URL: <https://www.unrealengine.com/en-US/tech-blog/an-early-look-at-next-generation-real-time-hair-and-fu>

[FHG21] FEI Y., HUANG Y., GAO M.: Principles towards real-time simulation of material point method on modern gpus. *arXiv preprint arXiv:2111.00699* (2021).

[Ger24] GERMANIDIS A.: Introducing gen-3 alpha: A new frontier for video generation. <https://runwayml.com/research/introducing-gen-3-alpha>, 2024. Runway Research.

[GGH\*25] GAO Y., GUO H., HOANG T., HUANG W., JIANG L., KONG F., LI H., LI J., LI L., LI X., ET AL.: Seedance 1.0: Exploring the boundaries of video generation models. *arXiv preprint arXiv:2506.09113* (2025).

[GHH\*24] GAO R., HOLYNSKI A., HENZLER P., BRUSSEE A., MARTIN-BRUALLA R., SRINIVASAN P., BARRON J. T., POOLE B.: Cat3d: Create anything in 3d with multi-view diffusion models. *arXiv preprint arXiv:2405.10314* (2024).

[Goo25] GOOGLE DEEPMIND: Veo — state-of-the-art video generation model. <https://deephind.google/models/veo/>, 2025. Google DeepMind.

[HCB\*24] HACOHEN Y., CHIPRUT N., BRAZOWSKI B., SHALEM D., MOSHE D., RICHARDSON E., LEVIN E., SHIRAN G., ZABARI N., GORDON O., ET AL.: Ltx-video: Realtime video latent diffusion. *arXiv preprint arXiv:2501.00103* (2024).

[HSW\*21] HU E. J., SHEN Y., WALLIS P., ALLEN-ZHU Z., LI Y., WANG S., WANG L., CHEN W.: Lora: Low-rank adaptation of large language models. arxiv 2021. *arXiv preprint arXiv:2106.09685* 10 (2021).

[HTG08] HUYNH-THU Q., GHANBARI M.: Scope of validity of psnr in image/video quality assessment. *Electronics letters* 44, 13 (2008), 800–801.

[Hu24] HU L.: Animate anyone: Consistent and controllable image-to-video synthesis for character animation. In *Proceedings of the IEEE/CVF Conference on Computer Vision and Pattern Recognition* (2024), pp. 8153–8163.

[HWP\*23] HSU J., WANG T., PAN Z., GAO X., YUKSEL C., WU K.: Sag-free initialization for strand-based hybrid hair simulation. *ACM Transactions on Graphics (TOG)* 42, 4 (2023), 1–14.

[HXG\*24] HE H., XU Y., GUO Y., WETZSTEIN G., DAI B., LI H., YANG C.: Cameractrl: Enabling camera control for text-to-video generation. *arXiv preprint arXiv:2404.02101* (2024).

[IMP\*13] IBEN H., MEYER M., PETROVIC L., SOARES O., ANDERSON J., WITKIN A.: Artistic simulation of curly hair. In *Proceedings of the 12th ACM SIGGRAPH/Eurographics Symposium on Computer Animation* (2013), pp. 63–71.

[JCW\*25] JIANG L., CHEN S., WU B., GUAN X., ZHANG J.: Vidsketch: Hand-drawn sketch-driven video generation with diffusion control. *arXiv preprint arXiv:2502.01101* (2025).

[KHWKS23] KARRAS J., HOLYNSKI A., WANG T.-C., KEMELMACHER-SHLIZERMAN I.: Dreampose: Fashion video synthesis with stable diffusion. In *Proceedings of the IEEE/CVF International Conference on Computer Vision* (2023), pp. 22680–22690.

[KLA19] KARRAS T., LAINE S., AILA T.: A style-based generator architecture for generative adversarial networks. In *Proceedings of the IEEE/CVF conference on computer vision and pattern recognition* (2019), pp. 4401–4410.

[KTZ\*24] KONG W., TIAN Q., ZHANG Z., MIN R., DAI Z., ZHOU J., XIONG J., LI X., WU B., ZHANG J., ET AL.: Hunyuanyvideo: A systematic framework for large video generative models. *arXiv preprint arXiv:2412.03603* (2024).

[LGC\*24] LIN B., GE Y., CHENG X., LI Z., ZHU B., WANG S., HE X., YE Y., YUAN S., CHEN L., ET AL.: Open-sora plan: Open-source large video generation model. *arXiv preprint arXiv:2412.00131* (2024).

[LGL\*25] LIANG R., GOJCIC Z., LING H., MUNKBERG J., HASSELGREN J., LIN C.-H., GAO J., KELLER A., VIJAYKUMAR N., FIDLER S., ET AL.: Diffusion renderer: Neural inverse and forward rendering with video diffusion models. In *Proceedings of the Computer Vision and Pattern Recognition Conference* (2025), pp. 26069–26080.

[LLC\*25] LIN G. W.-C., LARIONOV E., CHEN H.-Y., ROBLE D., STUYCK T.: Neuralocks: Real-time dynamic neural hair simulation. *arXiv preprint arXiv:2507.05191* (2025).

[LOZ\*24] LUO H., OUYANG M., ZHAO Z., JIANG S., ZHANG L., ZHANG Q., YANG W., XU L., YU J.: Gaussianhair: Hair modeling and rendering with light-aware gaussians. *arXiv preprint arXiv:2402.10483* (2024).

[MAZ\*24] MIAO K., AGRAWAL H., ZHANG Q., SEMERARO F., CAVALLO M., GU J., TOSHEV A.: Dsplats: 3d generation by denoising splats-based multiview diffusion models. *arXiv preprint arXiv:2412.09648* (2024).

[MHC\*24] MA Y., HE Y., CUN X., WANG X., CHEN S., LI X., CHEN Q.: Follow your pose: Pose-guided text-to-video generation using pose-free videos. In *Proceedings of the AAAI Conference on Artificial Intelligence* (2024), vol. 38, pp. 4117–4125.

[MJC\*03] MARSCHNER S. R., JENSEN H. W., CAMMARANO M., WORLEY S., HANRAHAN P.: Light scattering from human hair fibers. *ACM Transactions on Graphics (TOG)* 22, 3 (2003), 780–791.

[MWM08] MOON J. T., WALTER B., MARSCHNER S.: Efficient multiple scattering in hair using spherical harmonics. In *ACM SIGGRAPH 2008 papers*. 2008, pp. 1–7.

[Ope24] OPENAI: Sora. <https://openai.com/sora/>, 2024.

[PHA05] PETROVIC L., HENNE M., ANDERSON J.: Volumetric methods for simulation and rendering of hair. *Pixar Animation Studios* 2, 4 (2005), 1–6.

[Pik24] PIKA LABS: Tag: Pika 1.5 [blog posts: *Pika Labs 1.5 Video Generation Features*, *Pika 1.5 Pikaffects*]. <https://pikalabs.org/tag/pika-1-5/>, 2024. Pika Labs.

[PZB\*24] POLYAK A., ZOHAR A., BROWN A., TJANDRA A., SINHA A., LEE A., VYAS A., SHI B., MA C.-Y., CHUANG C.-Y., ET AL.: Movie gen: A cast of media foundation models. *arXiv preprint arXiv:2410.13720* (2024).

[RCTI91] ROSENBLUM R. E., CARLSON W. E., TRIPP III E.: Simulating the structure and dynamics of human hair: modelling, rendering and animation. *The Journal of Visualization and Computer Animation* 2, 4 (1991), 141–148.

[RWF\*25] ROSU R. A., WU K., FENG Y., ZHENG Y., BLACK M. J.: Difflocks: Generating 3d hair from a single image using diffusion models. In *Proceedings of the Computer Vision and Pattern Recognition Conference* (2025), pp. 10847–10857.

[SWY\*23] SHI Y., WANG P., YE J., LONG M., LI K., YANG X.: Mvdream: Multi-view diffusion for 3d generation. *arXiv preprint arXiv:2308.16512* (2023).

[THW\*25] TIAN L., HU S., WANG Q., ZHANG B., BO L.: Emo2: End-effector guided audio-driven avatar video generation. *arXiv preprint arXiv:2501.10687* (2025).

[TJW\*23] TANG L., JIA M., WANG Q., PHOO C. P., HARIHARAN B.: Emergent correspondence from image diffusion. *Advances in Neural Information Processing Systems* 36 (2023), 1363–1389.

[WBSS04] WANG Z., BOVIK A. C., SHEIKH H. R., SIMONCELLI E. P.: Image quality assessment: from error visibility to structural similarity. *IEEE transactions on image processing* 13, 4 (2004), 600–612.

[WGL06] WARD K., GALLOPPO N., LIN M. C.: A simulation-based vr system for interactive hairstyling. In *IEEE Virtual Reality Conference (VR 2006)* (2006), IEEE, pp. 257–260.

[WNS\*23] WANG Z., NAM G., STUYCK T., LOMBARDI S., CAO C., SARAGIH J., ZOLLHÖFER M., HODGINS J., LASSNER C.: Neuwigts: A neural dynamic model for volumetric hair capture and animation. In *Proceedings of the IEEE/CVF Conference on Computer Vision and Pattern Recognition* (2023), pp. 8641–8651.

[WWA\*25] WAN T., WANG A., AI B., WEN B., MAO C., XIE C.-W., CHEN D., YU F., ZHAO H., YANG J., ET AL.: Wan: Open and advanced large-scale video generative models. *arXiv preprint arXiv:2503.20314* (2025).

[WZG\*24] WANG X., ZHANG S., GAO C., WANG J., ZHOU X., ZHANG Y., YAN L., SANG N.: Unianimate: Taming unified video diffusion models for consistent human image animation. *arXiv preprint arXiv:2406.01188* (2024).

[WZT\*25] WANG X., ZHANG S., TANG L., ZHANG Y., GAO C., WANG Y., SANG N.: Unianimate-dit: Human image animation with large-scale video diffusion transformer. *arXiv preprint arXiv:2504.11289* (2025).

[XCL\*24] XU Y., CHEN B., LI Z., ZHANG H., WANG L., ZHENG Z., LIU Y.: Gaussian head avatar: Ultra high-fidelity head avatar via dynamic gaussians. In *Proceedings of the IEEE/CVF conference on computer vision and pattern recognition* (2024), pp. 1931–1941.

[XLX\*24] XING J., LIU H., XIA M., ZHANG Y., WANG X., SHAN Y., WONG T.-T.: Tooncrafter: Generative cartoon interpolation. *ACM Transactions on Graphics (TOG)* 43, 6 (2024), 1–11.

[YHW\*25] YE Z., HUANG H., WANG X., WAN P., ZHANG D., LUO W.: Stylemaster: Stylize your video with artistic generation and translation. In *Proceedings of the Computer Vision and Pattern Recognition Conference* (2025), pp. 2630–2640.

[YTZ\*24] YANG Z., TENG J., ZHENG W., DING M., HUANG S., XU J., YANG Y., HONG W., ZHANG X., FENG G., ET AL.: Cogvideox: Text-to-video diffusion models with an expert transformer. *arXiv preprint arXiv:2408.06072* (2024).

[YZYL23] YANG Z., ZENG A., YUAN C., LI Y.: Effective whole-body pose estimation with two-stages distillation. In *Proceedings of the IEEE/CVF International Conference on Computer Vision* (2023), pp. 4210–4220.

[ZIE\*18] ZHANG R., ISOLA P., EFROS A. A., SHECHTMAN E., WANG O.: The unreasonable effectiveness of deep features as a perceptual metric. In *Proceedings of the IEEE conference on computer vision and pattern recognition* (2018), pp. 586–595.

[ZJL\*23] ZHENG Y., JIN Z., LI M., HUANG H., MA C., CUI S., HAN X.: Hairstep: Transfer synthetic to real using strand and depth maps for single-view 3d hair modeling. In *Proceedings of the IEEE/CVF Conference on Computer Vision and Pattern Recognition* (2023), pp. 12726–12735.

[ZPY\*24] ZHENG Z., PENG X., YANG T., SHEN C., LI S., LIU H., ZHOU Y., LI T., YOU Y.: Open-sora: Democratizing efficient video production for all. *arXiv preprint arXiv:2412.20404* (2024).

[ZRA23] ZHANG L., RAO A., AGRAWALA M.: Adding conditional control to text-to-image diffusion models. In *Proceedings of the IEEE/CVF international conference on computer vision* (2023), pp. 3836–3847.

[ZYWK08] ZINKE A., YUKSEL C., WEBER A., KEYSER J.: Dual scattering approximation for fast multiple scattering in hair. In *ACM SIGGRAPH 2008 papers*. 2008, pp. 1–10.

[ZZS\*25] ZHANG Y., ZHANG Q., SONG Y., ZHANG J., TANG H., LIU J.: Stable-hair: Real-world hair transfer via diffusion model. In *Proceedings of the AAAI Conference on Artificial Intelligence* (2025), vol. 39, pp. 10348–10356.